Sayiter Yildiz[1],*
Gamze Topal Canbaz[2]
Savaş Kaya[3]
Mikhail M. Maslov[4]

Density Functional Theory Computations and Experimental Analyses to Highlight the Degradation of Reactive Black 5 Dye

The oxidative degradation of Reactive Black 5 (RB5) in aqueous solution was investigated using Fenton (FP), photo Fenton (P-FP), sono Fenton (S-FP), and sono photo Fenton (S-P-FP) processes. Degradation experiments showed efficient dye degradation for FP, P-FP, S-FP, and S-P-FP under optimal conditions. The half-life values of the reaction calculated for first-order reaction kinetics showed that the S-FP process is faster than the FP and P-FP processes. Using DFT calculations, the chemical reactivities of the studied chemical systems were analyzed. Especially the calculated chemical hardness values reflect the reactivities of the dye and the dye-Fe^{2+} complex. The calculated binding energy between the Fe^{2+} ion and RB5 of 15.836 eV is compatible with the prediction made in the light of the principle of hard and soft acids and bases. The computed data supported the experimental observations.

1 Introduction

Textile wastewater contains different types of dyes with low degradability [1]. In the case of azo dyes, there is a significant amount of residual dye in the wastewater due to losses in the dyeing process [2]. Most azo dyes are carcinogenic to humans and cause toxic effects in aquatic life [3]. Therefore, they must be removed from the water so that it does not cause adverse environmental and ecological effects [4]. However, conventional wastewater treatment plants cannot separate most of the dyes found in industrial wastewater [5].

Reactive Black 5 (RB5) is an azo dye widely used in textile dyeing [6]. RB5 can be degraded by different methods, including Fenton-like oxidation [7–10], photo-electrochemical process [11], adsorption [12–16], coagulation/flocculation [17, 18], photocatalysis [19, 20], ozonation [21], nanocomposites [22, 23], membrane filtration [24], and activated carbon [25, 26].

Advanced oxidation processes (AOPs) rely on strong oxidants such as hydroxyl radicals ($^{\bullet}OH$) and occur mainly in the presence of hydrogen peroxide (H_2O_2), transition metal ions, UV light, and an alkali or acid [27]. Fenton process (FP) efficiency depends on different operating parameters [28]. In the Fenton reaction, radical species ($HO_2^{\bullet}$, $^{\bullet}OH$) are formed by the reaction of H_2O_2 and iron catalyst [29]. The main chemical reactions in the formation of radical species are given in Eqs. (1) and (2) [30]:

$$H_2O_2 + Fe^{2+} \rightarrow Fe^{3+} + {}^{\bullet}OH + HO^- \tag{1}$$

$$Fe^{2+} + {}^{\bullet}OH \rightarrow Fe^{3+} + OH^- \tag{2}$$

According to Eq. (1), $^{\bullet}OH$ production occurs in a quick reaction. However, it can be oxidized because of the reaction of Fe^{2+} with $^{\bullet}OH$ [Eq. (2)] [31]. During the reaction, $^{\bullet}OH$ rapidly attacks organic substrates [32].

The reactive treatment of FP with UV light (photo Fenton) directly affects the formation of $^{\bullet}OH$ radicals, and can be an alternative for dye degradation [33]. In the photo Fenton process (P-FP), $^{\bullet}OH$ formation occurs by the following reactions (Eqs. (3) and (4)) [34]:

$$H_2O_2 + UV \rightarrow {}^{\bullet}OH + {}^{\bullet}OH \tag{3}$$

[1]Assoc. Prof. Sayiter Yildiz
(sayiteryildiz@gmail.com)
Sivas Cumhuriyet University, Engineering Faculty, Department of Environmental Engineering, 58140, Sivas, Turkey.

[2]Dr. Gamze Topal Canbaz
Sivas Cumhuriyet University, Engineering Faculty, Department of Chemical Engineering, 58140, Sivas, Turkey.
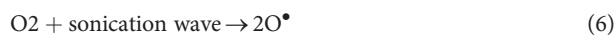
[3]Assoc. Prof. Savaş Kaya
Sivas Cumhuriyet University, Health Services Vocational School, Department of Pharmacy, 58140, Sivas, Turkey.

[4]Prof. Mikhail M. Maslov
National Research Nuclear University, MEPhI Department of Condensed Matter Physics, Kashirskoe Shosse 31, 115409, Moscow, Russia.

$$Fe^{3+} + H_2O + UV \rightarrow {}^\bullet OH + Fe^{2+} + H^+ \qquad (4)$$
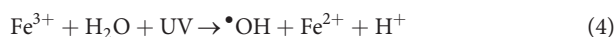
Combining FP with ultrasonic irradiation (sono-photo Fenton) can accelerate the degradation reaction with the synergistic effect it creates [35]. Sono-photo Fenton (S-P-FP) reaction mechanisms are described by (Eqs. (5)–(7)) [36].

$$H_2O_2 + \text{sonication wave} \rightarrow 2{}^\bullet OH \qquad (5)$$

$$O2 + \text{sonication wave} \rightarrow 2O^\bullet \qquad (6)$$

$$O^\bullet + H_2O \rightarrow 2{}^\bullet OH \qquad (7)$$

In this study, the degradation performance of RB5 by Fenton-like reactions was investigated under different reaction conditions. The electronic structure was calculated using density functional theory (DFT). For process performance, the variations in degradation efficiency due to variables such as amount of Fenton reagents, reaction time, initial pH, different UV light sources, and dye concentration were investigated. This study is especially important in terms of examining the interaction between Fenton reagents and dye molecules with DFT. The novelty of this work is that the degradation of RB5 was studied comparatively and the degradation mechanism was highlighted in the light of DFT computations.

2 Materials and Methods

2.1 Experimental Study

H_2O_2 (35%) and Fe^{2+} ($FeSO_4 \cdot 7H_2O$) were used to initiate Fenton redox reactions and generate ${}^\bullet OH$ radicals. Since RB5 is one of the most widely used azo dyes in the textile industry [4], it was chosen for this study. Synthetic wastewater was prepared using RB5 obtained from Sigma-Aldrich. Fig. 1 shows the UV-Vis absorption spectrum and chemical structure of RB5 [37].
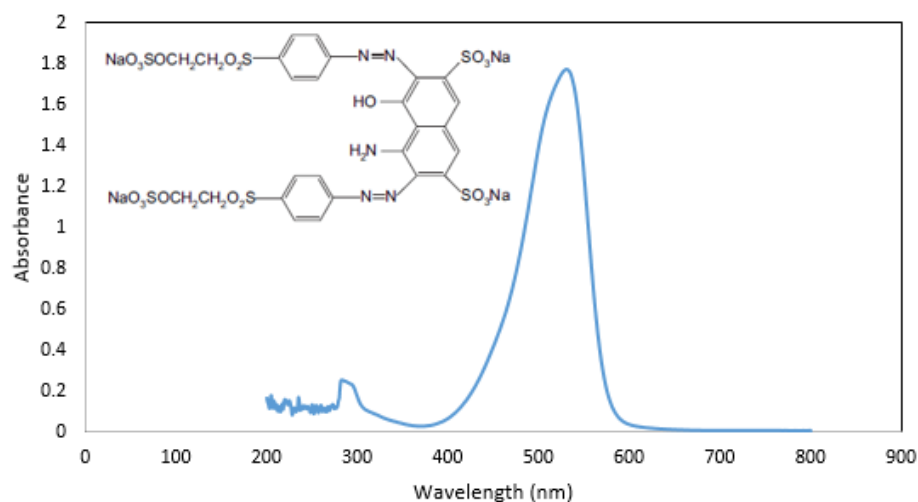

Figure 1. UV-Vis absorption spectrum and chemical structure of RB5

In the study, UVA (365 nm), UVB (302 nm), and UVC (256 nm) light sources and ultrasound with a frequency of 40 kHz and a power of 180 W were used. Dye values were determined with a spectrophotometer [38]. The dye degradation efficiency η_{dye} was calculated by Eq. (8) [39].

$$\eta_{dye} = \frac{C_0 - C_t}{C_0} \times 100 \% \qquad (8)$$

where C_0 and C_t are the initial RB5 concentration and the RB5 concentration at time t, respectively.

2.2 DFT Calculations

The Perdew-Burke-Ernzerhof (GGA-PBE) exchange-correlation functional [40] and hybrid electronic basis set combining 6-31G(d) [41] and 6-31G elements and 6-31G*-LDZ [42] (for Fe) were used in the calculations. TeraChem software [43–46] was used as a graphics processor-based electronic structure package. The efficient geoMETRIC energy minimizer was used in geometry optimization. D3 dispersion corrections [48] were included to account for weak noncovalent interactions. The mathematical relations proposed for chemical potential μ, electronegativity χ, chemical hardness η, and chemical softness σ in Conceptual DFT are given below (Eqs. (9)–(11)) [49].

$$\mu = -\chi = \left[\frac{\partial E}{\partial N}\right]_{v(r)} \qquad (9)$$

$$\eta = \left[\frac{\partial \mu}{\partial N}\right]_{v(r)} = \left[\frac{\partial^2 E}{\partial N^2}\right]_{v(r)} \qquad (10)$$

$$\sigma = \frac{1}{\eta} \qquad (11)$$

To derive these relationships, a parabolic curve is used that shows the connection between total electronic energy E and the total number of electrons N of a chemical system. To apply the finite differences approach to the parabolic relationship, the aforementioned identifiers are related to the ionization energy I and electron affinity A of the atomic and molecular chemical systems (Eqs. (12)–(14)) [50, 51]:

$$\mu = -\chi = -\left(\frac{I + A}{2}\right) \qquad (12)$$

$$\eta = I - A \qquad (13)$$

$$\sigma = \frac{1}{I - A} \qquad (14)$$

Another popular parameter for chemical reactivity analysis is the

Chem. Eng. Technol. **2023**, *46*, No. 10, 2133–2140

© 2023 Wiley-VCH GmbH

www.cet-journal.com

electrophilicity index ω [52], which is mathematically presented as Eq. (15):

$$\omega = \frac{\chi^2}{2\eta} = \frac{\mu^2}{2\eta} \tag{15}$$

The equations for the calculation of the electron-donating power and electron-accepting power parameters introduced by Gazquez and co-workers [53] are presented as Eqs. (16) and (17):

$$\omega^- = \frac{(3I + A)^2}{16(I - A)} \tag{16}$$

$$\omega^+ = \frac{(I + 3A)^2}{16(I - A)} \tag{17}$$

In this study, the aforementioned descriptors were calculated for the studied chemical systems because dye degradation processes are closely relevant to the chemical reactivity of the considered dyes. The Koopmans theorem [54] was used to estimate the ionization energy and electron affinities of the chemical systems used in the study.

3 Results and Discussion

3.1 Degradation of RB5

Degradation experiments on RB5 were carried out under (1) dye + Fe^{2+} + H_2O_2 (FP), (2) dye + Fe^{2+} + H_2O_2 + UV (P-FP), (3) dye + Fe^{2+} + H_2O_2 + US (S-FP), and (4) dye + Fe^{2+} + H_2O_2 + UV + US (S-P-FP) conditions (Fig. 2). In the study, Fe^{2+} concentration was 10 mg L^{-1}, H_2O_2 concentration 75 mg L^{-1}, pH 3, RB5 concentration 100 mg L^{-1}, and equilibrium was reached in the first 30 min. A Fenton process occurs in two stages. The first one is called the Fe^{2+}/H_2O_2 stage and it breaks down the azo bonds (N=N) by $^\bullet$OH very quickly, since they are easier to destroy than aromatic ring structures. The second stage is the Fe^{3+}/H_2O_2 stage. The oxidation rate in this stage is lower than in the first stage. Therefore, complete mineralization cannot be achieved in this stage [55]. In the first stage of the Fenton reaction, Fe^{2+} reacts with hydrogen peroxide and turns into Fe^{3+} [56].

The η_{dye} value was 97.1, 98.24, 97.73, 97.93, 97.42, 96.22, 96.08, and 96.19 % in FP, P-FP (for UVA, UVB, and UVC), S-FP, and S-P-FP (for UVA, UVB, and UVC), respectively. While η_{dye} was quite high in all processes, the highest efficiency of 98.24 % was obtained in P-FP with a UVA lamp. Bhaumik et al. [57] studied the catalytic degradation of RB5 using Fe^0/TiO_2 nanocomposites, and the RB5 removal efficiency of the mentioned composite material was determined to be 97.33 %. It is noteworthy that our method also provides such high efficiency for the removal of RB5.
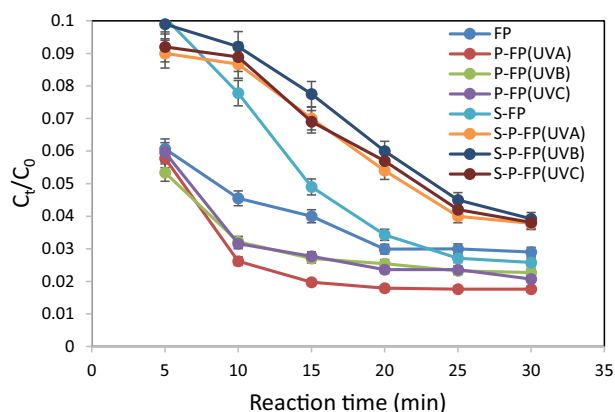

Figure 2. Degradation of RB5 under different reaction conditions.

3.2 Effect of pH on Degradation

To determine the effect of pH, degradation was investigated in the pH range of 2–7 (Fe^{2+} 10 mg L^{-1}, H_2O_2 75 mg L^{-1}, t = 30 min, and RB5 100 mg L^{-1}; Fig. 3). Different studies have shown that low pH promotes dye degradation [58, 59]. pH is an effective parameter in the formation of $^\bullet$OH [60]. An acidic environment increases radical formation and oxidation [61]. H_2O_2 is also unstable and can decompose in alkaline solution, losing its oxidation ability. Therefore, H_2O_2 and Fe^{2+} ions have difficulty forming an effective redox system. In this case, the reagents become less effective in dye degradation [62].

In this study, the highest η_{dye} (97.1%) was obtained at pH 3. The η_{dye} value for RB5 was 96.9 % at pH 2, 97 % at pH 4, 95.9 at pH 5, 94.7 % at pH 6, and 93.5 % at pH 7.

3.3 Effect of Dye Concentration on Degradation

The effect of initial dye concentrations on η_{dye} is given in Fig. 3. The initial H_2O_2 concentration was adjusted to 100 mg L^{-1} and that of Fe^{2+} to 10 mg L^{-1}. The degradation effect was investi-

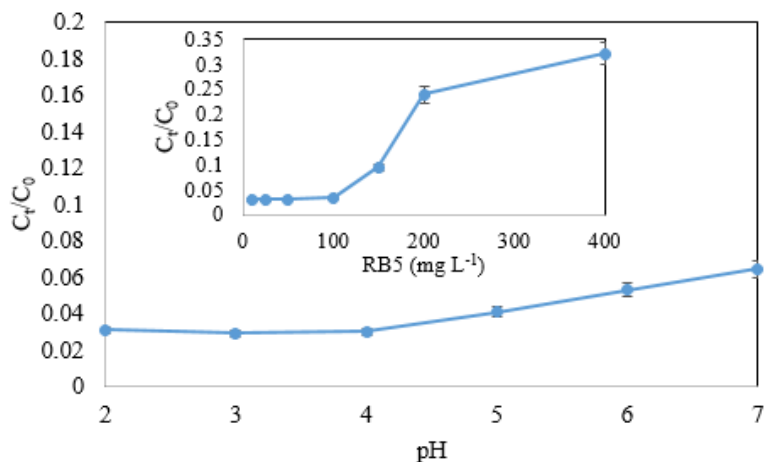**Figure 3.** Effect of pH and RB5 concentration on degradation.

gated by changing the RB5 concentration to 10, 25, 50, 100, 150, 200, and 400 mg L^{-1}. The η_{dye} values obtained for each concentration were calculated as 97.1, 97, 97, 96.7, 90.6, 75.9, and 67.8%, respectively. With increasing dye concentration the number of dye molecules increases, but the rate of degradation decreases, as the amount of $^{\bullet}$OH remains the same [33]. Also, high concentrations block active catalyst sites, reducing the production of active radicals. Different researchers have reported similar results to those obtained in this study [63, 64].

3.4 Effect of Fenton Reagents on Degradation

The amount of reagents used in the Fenton-like process plays an important role in terms of degradation efficiency [65]. The effect of different H_2O_2 concentrations (10, 25, 50, 75, 100, 150, 200, 300, 400 mg L^{-1}) and Fe^{2+} concentrations (10, 25, 50, 75, 100, 200, 400) was investigated (Fig. 4). Other conditions were t = 30 min, RB5 100 mg L^{-1}, pH 3 and Fe^{2+} 50 mg L^{-1} in the H_2O_2 study, and H_2O_2 100 mg L^{-1} in the Fe^{2+} study.

In the Fenton process, Fe^{2+} consumption occurs faster than its reproduction [66]. For this reason, a sufficient amount of Fe^{2+} is required to ensure continuous $^{\bullet}$OH production [67]. In addition, due to the scavenging effect [Eq. (2)] of Fe^{2+} at high concentrations on $^{\bullet}$OH [Eq. (9)] [68], η decreases with Fe^{2+} concentration [69]. The degradation efficiency was determined to be 97.1 % at 10 mg L^{-1} Fe^{2+} and this was the highest η_{dye} value obtained for Fe^{2+}. The η_{dye} value was 97 % in 50 mg L^{-1} Fe^{2+}, 90 % in 100 mg L^{-1} Fe^{2+}, 76 % in 200 mg L^{-1} Fe^{2+}, and 67.8 % in 400 mg L^{-1} Fe^{2+}.

The results showed that increasing the concentration of H_2O_2 partially increases the removal efficiency and then decreases it. The highest degradation efficiency was 97.2 % at 75 mg L^{-1} H_2O_2. The η_{dye} values for 10, 50, 100, 200, 300, and 400 mg L^{-1} H_2O_2 were 90, 96, 97.1, 97, 96.4, and 96 %, respectively. This result is consistent with the data obtained in other studies [70]. The effect of low concentrations of H_2O_2 on the system can be explained by the reduction in dye degradation efficiency with the formation of small amounts of $^{\bullet}$OH radicals.
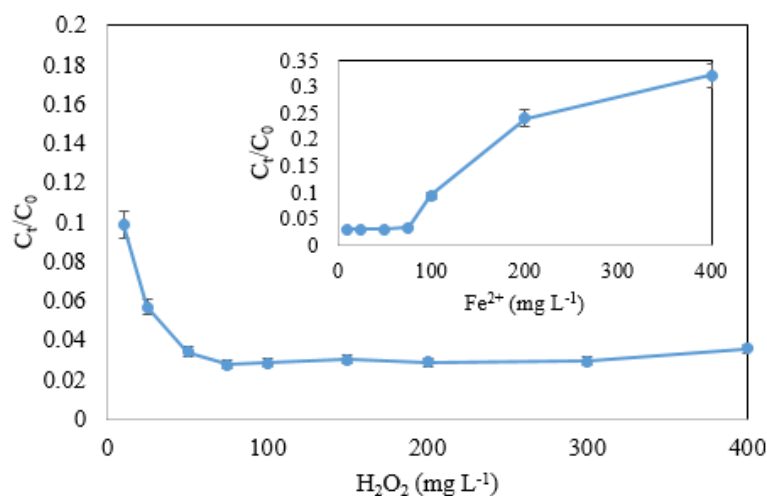
However, at high H_2O_2 concentrations, undesirable parallel reactions can occur, leading to the formation of H_2O and O_2 [71]. In addition, due to the large amount of H_2O_2, $^{\bullet}$OH radicals are consumed to generate hydroperoxyl radicals ($^{\bullet}$OOH, E^o = 1.42 V), which offer a lower reduction potential compared to the $^{\bullet}$OH radical (E^o = 2.80 V) (Eq. (18)), and thus adversely affect the process [72].

$$^{\bullet}OH + H_2O_2 \rightarrow {}^{\bullet}OOH + H_2O \tag{18}$$

3.5 Degradation Kinetics

The kinetics of the degradation of RB5 by Fenton-like reactions was investigated for zeroth-order, first-order, and second-order reactions according to time-dependent degradation (Eqs. (19)–(21)) [73, 74].

Zeroth-order kinetics:

$$C_t - C_0 = k_0 t \tag{19}$$

First-order kinetics:

$$\ln\left(\frac{C_0}{C_t}\right) = k_1 t \tag{20}$$

Second-order kinetics:

$$\frac{1}{C_t} - \frac{1}{C_0} = k_2 t \tag{21}$$

where k_0, k_1, and k_2 are the apparent kinetic rate constants of zeroth-, first-, and second-order reaction kinetics, respectively.

For first order reaction kinetics, the half-life of the reaction $t_{1/2}$ was calculated (Tab. 1). The $t_{1/2}$ values indicate that S-FP ($t_{1/2}$ = 103 min) was faster than the other Fenton processes ($t_{1/2}$ = 247–630 min).

RB5 degradation can be better explained by a zeroth-order kinetic model, for which the highest R^2 values are obtained. An increase in k was observed in processes using ultrasound (S-FP, S-P-FP). While the k_0 value was 0.122 mg L min^{-1} in FP and 0.130, 0.104, and 0.127 mg L min^{-1} in the UVA, UVB, and UVC processes, respectively, it was calculated to 0.601 mg L min^{-1} in S-FP. In S-P-FP, on the other hand, for different UV lamps it was 0.238, 0.261, and 0.241 mg L min^{-1}, respectively. The highest first-order kinetic constant k_1 was obtained with S-FP (0.0067). The fact that the S-FP is a faster process as determined by the $t_{1/2}$ calculation and the increase in k_1 can be explained by the increase in temperature with the use of ultrasound [74].

3.6 DFT Calculations

In this study, the effect of Fe^{2+} ion and H_2O_2 molecules on the geometry and electronic structure of RB5 was analyzed. The obtained results show that

Figure 4. Effect of Fenton reagents.

Table 1. Kinetic constants.

Process	Zeroth-order kinetics		First-order kinetics		Second-order kinetics		$t_{1/2}$ [min]
	k_0 [mg L min^{-1}]	R^2	k_1 [min^{-1}]	R^2	k_2 [mg L min^{-1}]	R^2	
FP	0.122	0.85	0.0013	0.84	-1×10^{-5}	0.84	533
P-FP (UV-A)	0.130	0.60	0.0014	0.59	-1×10^{-5}	0.58	495
P-FP (UV-B)	0.104	0.69	0.0011	0.69	-1×10^{-5}	0.69	630
P-FP (UV-C)	0.127	0.68	0.0013	0.67	-1×10^{-5}	0.67	533
S-FP	0.601	0.76	0.0067	0.74	-7×10^{-5}	0.72	103
S-P-FP (UV-A)	0.238	0.96	0.0025	0.96	-3×10^{-5}	0.96	277
S-P-FP (UV-B)	0.261	0.98	0.0028	0.98	-3×10^{-5}	0.98	247
S-P-FP (UV-C)	0.241	0.97	0.0026	0.97	-3×10^{-5}	0.96	266

sible". FP is thus useful to investigate the degradation of soft compounds, e.g., reactive dye. In stable states, polarizability is minimized while chemical hardness is maximized. The dipole moment is a measure of polarizability. It is clear from the calculations that RB5 is a soft dye ($\eta = 1.434$ eV). As a result of the interaction of RB5 with Fe^{2+}, a softer system with a chemical hardness of 0.113 is formed. In this way, the degradation process gets easier. The atomic structure, highest occupied molecular orbitals (HOMOs), and LUMOs of the calculated chemical systems are

the Fe ion distorts the structure of RB5 more strongly than hydrogen peroxide (see Figs. 5–7), and this can lead to further degradation. Fe^{2+} binds to the carbon atom belonging to the six-membered ring and oxygen atoms from the SO$_3$Na group. The H$_2$O$_2$ molecule is located closer to the SO$_3$Na group, weakly binding to the oxygen atom, and practically does not distort the carbon rings. In addition, the ion facilitates charge transfer by changing the electronic structure of the dye. It also significantly reduces the gap between the frontier orbitals (see Tab. 2). Note that the lowest unoccupied molecular orbital (LUMO) is localized just near the iron ion. In addition, the binding energies of Fe^{2+} and H$_2$O$_2$ were calculated according to Eqs. (22) and (23).
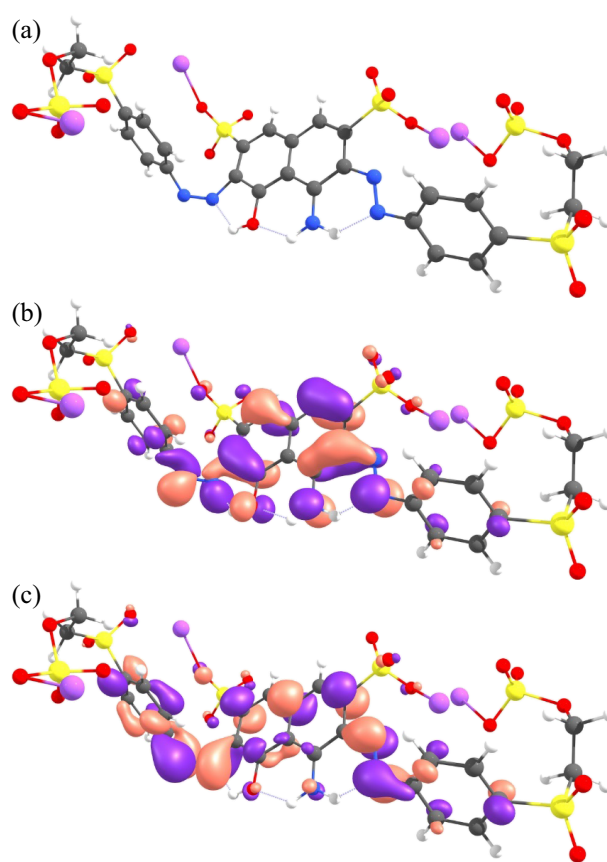
$$E_b = E\left(Fe^{2+}\right) + E(RB5) - E\left(RB5/Fe^{2+}\right) \qquad (22)$$

$$E_b = E(H_2O_2) + E(RB5) - E(RB5/H_2O_2) \qquad (23)$$

As can be seen from the binding energies E_b listed in Tab. 2, the Fe^{2+} ion binds much more strongly to RB5 than to H$_2$O$_2$.

Popular chemical parameters of Conceptual DFT provide great facilities to theoretical chemists in terms of reactivity analysis. Chemical hardness is the resistance of compounds to electron cloud polarization and is an important indicator of stability [76, 77]. According to the principle of hard and soft acids and bases (HSAB) [78], "hard acids prefer to adapt to hard bases and soft acids to soft bases." Soft chemicals exhibit high polarization and tend to undergo covalent interactions. The maximum hardness principle [79] states that "it is a law of nature that molecules arrange themselves to be as rigid as pos-

Figure 5. RB5: atomic structure (a), HOMO (b), and LUMO (c).

Table 2. Calculated electronic characteristics.

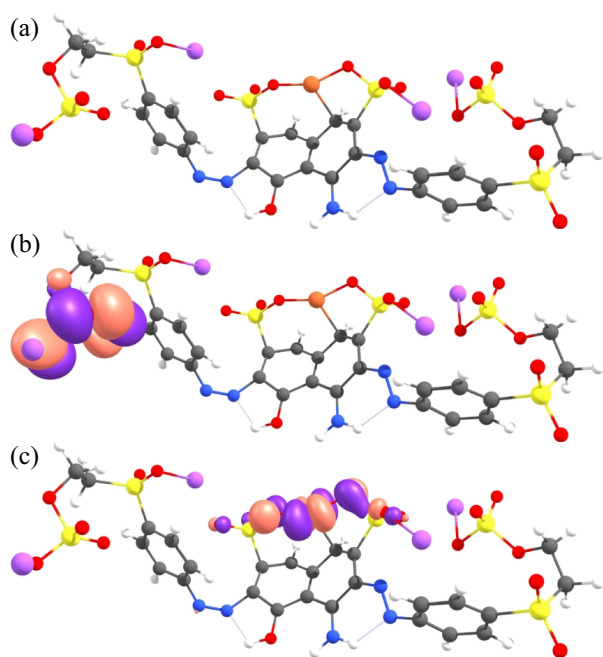| System	Dipole moment [Debye]	HOMO [eV]	LUMO [eV]	η [eV]	χ [eV]	ω [eV]	ω^- [eV]	ω^+ [eV]	E_b [eV]
RB5	10.948	−4.993	−3.559	1.434	4.276	6.38	14.98	10.70	–
RB5/Fe^{2+}	9.977	−9.750	−9.617	0.133	9.684	352.52	709.89	700.21	15.836
RB5/H$_2$O$_2$	21.533	−4.996	−3.703	1.293	4.350	7.32	16.89	12.54	0.941

Figure 6. RB5/Fe^{2+} complex: atomic structure (a), HOMO (b), and LUMO (c).
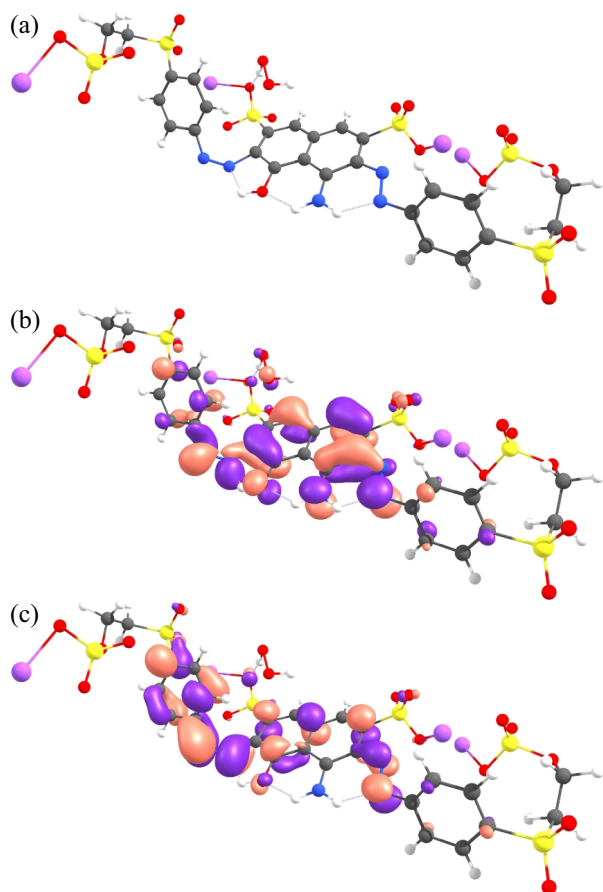

Figure 7. RB5/H_2O_2 complex: atomic structure (a), HOMO (b), and LUMO (c).

shown in Figs. 5–7. The theoretical results are in good agreement with the experimental results. The calculated binding energies support the HSAB principle.

4 Conclusion

Degradation of RB5 was carried out under different experimental conditions. Fenton oxidation was carried out under optimum conditions of 75 mg L^{-1} H_2O_2, 10 mg L^{-1} Fe^{2+}, 100 mg L^{-1} RB5, pH 3, and t = 30 min. The η_{dye} value in FP was 97.1 %. In P-FP, in which UVA, UVB, and UVC light were used, η_{dye} values of 98.24, 97.73, and 97.93 %, respectively, were obtained. In S-P-FP, the η_{dye} values for UVA, UVB, and UVC light were 96.22, 96.08, and 96.19 %, respectively. In S-FP, the removal efficiency was 97.42 %. Also, the calculated $t_{1/2}$ values showed that the S-FP process ($t_{1/2}$ = 103 min) was faster than the FP and P-FP processes ($t_{1/2}$ = 495, 533, 630 min). The computed Conceptual DFT parameters are in good agreement with the experiments. The results support the maximum hardness principle and HSAB principle. Fenton-like processes could be a very promising technology for removing RB5 dye from wastewater. In the light of the comparisons with the papers published in the literature, it can be said that the experimental method used here provides high efficiency for the removal of RB5.

The authors have declared no conflict of interest.

Symbols used

A	[eV]	electron affinity
C_t	[mg L^{-1}]	RB5 concentration at time t
C_0	[mg L^{-1}]	initial RB5 concentration
E	[eV]	total electronic energy
E^o	[V]	reduction potential
E_b	[eV]	binding energy
I	[ev]	ionization energy
k_0	[mg L min^{-1}]	zeroth-order rate constant
k_1	[min^{-1}]	first-order rate constant
k_2	[mg L min^{-1}]	second-order rate constant
N	[–]	total number of electrons
$t_{1/2}$	[min]	half-life

Greek letters

η_{dye}	[%]	dye degradation efficiency
η	[eV]	chemical hardness
μ	[eV]	chemical potential
σ	[eV]	chemical softness
χ	[eV]	electronegativity
ω	[eV]	electrophilicity index
ω^-	[eV]	electron-donating power
ω^+	[eV]	electron-accepting power

Abbreviations

AOP	advanced oxidation process
DFT	density functional theory

FP	Fenton process
HOMO	highest occupied molecular orbital
HSAB	hard and soft acids and bases
LUMO	highest occupied molecular orbital
P-FP	photo Fenton process
RB5	Reactive Black 5
S-FP	sono Fenton process
S-P-FP	sono photo Fenton process

References

[1] M. El Bouraie, W. S. El Din, *Sustainable Environ. Res.* **2016**, *26*, 209–216. DOI: https://doi.org/10.1016/j.serj.2016.04.014

[2] A. Alinsafi, M. Khemis, M. N. Pons, J. P. Leclerc, A. Yaacoubi, A. Benhammou, A. Nejmeddine, *Chem. Eng. Process. Process Intensif.* **2005**, *44*, 461–470. DOI: https://doi.org/10.1016/j.cep.2004.06.010

[3] S. Chatterjee, S. R. Lim, S. H. Woo, *Chem. Eng. J.* **2010**, *160*, 27–32. DOI: https://doi.org/10.1016/j.cej.2010.02.045

[4] S. Şahinkaya, *J. Ind. Eng. Chem.* **2013**, *19*, 601–605. DOI: https://doi.org/10.1016/j.jiec.2012.09.023

[5] E. Brillas, C. A. Martínez-Huitle, *Appl. Catal. B Environ.* **2015**, *166–167*, 603–643. DOI: https://doi.org/10.1016/j.apcatb.2014.11.016

[6] J. E. B. McCallum, S. A. Madison, S. Alkan, R. L. Depinto, R. U. Rojas Wahl, *Environ. Sci. Technol.* **2000**, *34*, 5157–5164. DOI: https://doi.org/10.1021/es0008665

[7] R. Salazar, M. S. Ureta-Zañartu, *J. Chil. Chem. Soc.* **2012**, *57*, 999–1003. DOI: https://doi.org/10.4067/S0717-97072012000100010

[8] F. Iranpour, H. Pourzamani, N. Mengelizadeh, P. Bahrami, H. Mohammadi, *J. Environ. Chem. Eng.* **2018**, *6*, 3418–3435. DOI: https://doi.org/10.1016/j.jece.2018.05.023

[9] M. B. K. Suhan, S. B. Shuchi, A. Anis, Z. Haque, M. S. Islam, *Environ. Nanotechnol. Monit. Manag.* **2020**, *14*, 100335. DOI: https://doi.org/10.1016/j.enmm.2020.100335

[10] J. Domenzain-Gonzalez, J. J. Castro-Arellano, L. A. Galicia-Luna, M. Rodriguez-Cruz, R. T. Hernandez-Lopez, L. Lartundo-Rojas, *J. Environ. Chem. Eng.* **2021**, *9*, 105281. DOI: https://doi.org/10.1016/j.jece.2021.105281

[11] M. Riera-Torres, C. Gutiérrez-Bouzán, *Sep. Purif. Technol.* **2012**, *98*, 375–382. DOI: https://doi.org/10.1016/j.seppur.2012.08.005

[12] M. Bhaumik, R. I. McCrindle, A. Maity, S. Agarwal, V. K. Gupta, *J. Colloid Interface Sci.* **2016**, *466*, 442–451. DOI: https://doi.org/10.1016/j.jcis.2015.12.056

[13] S. Ziane, F. Bessaha, K. Marouf-Khelifa, A. Khelifa, *J. Mol. Liq.* **2018**, *249*, 1245–1253. DOI: https://doi.org/10.1016/j.molliq.2017.11.130

[14] J. C. Coura, D. Profeti, L. P. R. Profeti, *Mater. Chem. Phys.* **2020**, *256*, 123711. DOI: https://doi.org/10.1016/j.matchemphys.2020.123711

[15] M. M. Felista, W. C. Wanyonyi, G. Ongera, *Sci. African* **2020**, *7*, e00283. DOI: https://doi.org/10.1016/j.sciaf.2020.e00283

[16] V. H. Vargas, R. R. Paveglio, P. de S. Pauletto, N. P. G. Salau, L. G. Dotto, *Chem. Eng. Commun.* **2020**, *207*, 523–536. DOI: https://doi.org/10.1080/00986445.2019.1605362

[17] C. S. Miyashiro, G. A. P. Mateus, T. R. T. dos Santos, M. P. Paludo, R. Bergamasco, M. R. Fagundes-Klen, *Mater. Sci. Eng. C* **2021**, *119*, 111523. DOI: https://doi.org/10.1016/j.msec.2020.111523

[18] N. de C. L. Beluci, G. A. P. Mateus, C. S. Miyashiro, N. C. Homem, R. G. Gomes, M. R. Fagundes-Klen, R. Bergamasco, A. M. S. Vieira, *Sci. Total Environ.* **2019**, *664*, 222–229. DOI: https://doi.org/10.1016/j.scitotenv.2019.01.199

[19] M. N. Chong, Y. J. Cho, P. E. Poh, B. Jin, *J. Cleaner Prod.* **2015**, *89*, 196–202. DOI: https://doi.org/10.1016/j.jclepro.2014.11.014

[20] F. Liu, X. Wang, Z. Liu, F. Miao, Y. Xu, H. Zhang, *Sep. Purif. Technol.* **2021**, *279*, 119754. DOI: https://doi.org/10.1016/j.seppur.2021.119754

[21] N. P. Chokshi, J. P. Ruparelia, *Ozone Sci. Eng.* **2022**, *44*, 182–195. DOI: https://doi.org/10.1080/01919512.2021.1901070

[22] A. Mohagheghian, R. Vahidi-Kolur, M. Pourmohseni, J. K. Yang, M. Shirzad-Siboni, *Water Air Soil Pollut.* **2015**, *226 (9)*, 1–16. DOI: https://doi.org/10.1007/s11270-015-2539-7

[23] M. E. Mahmoud, M. F. Amira, S. M. Seleim, G. M. Nabil, M. E. Abouelanwar, *J. Nanostruct. Chem.* **2021**, *11*, 645–662. DOI: https://doi.org/10.1007/s40097-021-00390-0

[24] L. Semiz, *Polym. Bull.* **2020**, *77*, 3047–3059. DOI: https://doi.org/10.1007/s00289-019-02896-8

[25] R. Singh, P. V. Nidheesh, T. Sivasankar, *Environ. Eng. Manag. J.* **2019**, *18*, 2335–2342. DOI: https://doi.org/10.30638/eemj.2019.222

[26] N. A. F. Abd Latif, A. H. Nordin, N. Ngadi, W. Nabgan, M. Jusoh, Z. Mohamad, M. G. Mohd Nawawi, *Mater. Today Proc.* **2021**, *47*, 1241–1245. DOI: https://doi.org/10.1016/j.matpr.2021.02.331

[27] A. Mohey El-Dein, J. A. Libra, U. Wiesmann, *Chemosphere* **2003**, *52*, 1069–1077. DOI: https://doi.org/10.1016/S0045-6535(03)00226-1

[28] S. Meriç, D. Kaptan, T. Ölmez, *Chemosphere* **2004**, *54*, 435–441. DOI: https://doi.org/10.1016/j.chemosphere.2003.08.010

[29] S. S. Lin, M. D. Gurol, *Environ. Sci. Technol.* **1998**, *32*, 1417–1423. DOI: https://doi.org/10.1021/es970648k

[30] K. Rajeshwar, J. G. Ibanez, *Environmental Electrochemistry*, Elsevier, **1997**.

[31] M. L. Kremer, *Phys. Chem. Chem. Phys.* **1999**, *1*, 3595–3605. DOI: https://doi.org/10.1039/a903915e

[32] F. J. Benitez, J. Beltran-Heredia, J. L. Acero, F. J. Rubio, *Chemosphere* **2000**, *41*, 1271–1277. DOI: https://doi.org/10.1016/S0045-6535(99)00536-6

[33] J. Feng, X. Hu, P. L. Yue, H. Y. Zhu, G. Q. Lu, *Water Res.* **2003**, *37*, 3776–3784. DOI: https://doi.org/10.1016/S0043-1354(03)00268-9

[34] M. S. Lucas, J. A. Peres, *Dyes Pigments* **2007**, *74*, 622–629. DOI: https://doi.org/10.1016/j.dyepig.2006.04.005

[35] B. Chen, X. Wang, C. Wang, W. Jiang, S. Li, *Ultrason. Sonochem.* **2011**, *18*, 1091–1096. DOI: https://doi.org/10.1016/j.ultsonch.2011.03.026

[36] J. Liang, S. Komarov, N. Hayashi, E. Kasai, *Ultrason. Sonochem.* **2007**, *14*, 201–207. DOI: https://doi.org/10.1016/j.ultsonch.2006.05.002

[37] P. M. Pérez García, S. L. Ibáñez-Calero, *Invest. Desarrolo* **2017**, *17*, 43–53. DOI: https://doi.org/10.23881/idupbo.017.1-4i

[38] APHA (American Public Health Association), Standard Methods for the Examination of Water and Wastewater, Standard Methods, **1998**, 541.

[39] J. Zhang, M. Yan, G. Sun, X. Li, K. Liu, *J. Alloys Compd.* **2022**, *889*, 161673. DOI: https://doi.org/10.1016/j.jallcom.2021.161673

[40] J. P. Perdew, K. Burke, M. Ernzerhof, *Phys. Rev. Lett.* **1996**, *77*, 3865–3868. DOI: https://doi.org/10.1103/PhysRevLett.77.3865

[41] W. J. Hehre, K. Ditchfield, J. A. Pople, *J. Chem. Phys.* **1972**, *56*, 2257–2261. DOI: https://doi.org/10.1063/1.1677527

[42] P. J. Hay, W. R. Wadt, *J. Chem. Phys.* **1985**, *82*, 299–310. DOI: https://doi.org/10.1063/1.448975

[43] I. S. Ufimtsev, T. J. Martinez, *J. Chem. Theory Comput.* **2009**, *5*, 2619–2628. DOI: https://doi.org/10.1021/ct9003004

[44] A. V. Titov, I. S. Ufimtsev, N. Luehr, T. J. Martinez, *J. Chem. Theory Comput.* **2013**, *9*, 213–221. DOI: https://doi.org/10.1021/ct300321a

[45] J. Kästner, J. M. Carr, T. W. Keal, W. Thiel, A. Wander, P. Sherwood, *J. Phys. Chem. A* **2009**, *113*, 11856–11865. DOI: https://doi.org/10.1021/jp9028968

[46] T. P. M. Goumans, C. R. A. Catlow, W. A. Brown, J. Kästner, P. Sherwood, *Phys. Chem. Chem. Phys.* **2009**, *11*, 5431–5436. DOI: https://doi.org/10.1039/b816905e

[47] L. P. Wang, C. Song, *J. Chem. Phys.* **2016**, *144 (21)*, 214108. DOI: https://doi.org/10.1063/1.4952956

[48] S. Grimme, J. Antony, S. Ehrlich, H. Krieg, *J. Chem. Phys.* **2010**, *132*, 154104. DOI: https://doi.org/10.1063/1.3382344

[49] Y. Kaya, A. Erçağ, G. Serdaroğlu, S. Kaya, I. B. Grillo, G. B. Rocha, *J. Mol. Struct.* **2021**, *1244*, 131224. DOI: https://doi.org/10.1016/j.molstruc.2021.131224

[50] *Conceptual Density Functional Theory and Its Application in the Chemical Domain* (Eds: N. Islam, S. Kaya), Apple Academic Press, **2018**. DOI: https://doi.org/10.1201/b22471

[51] S. Kaya, P. Banerjee, S. K. Saha, B. Tüzün, C. Kaya, *RSC Adv.* **2016**, *6*, 74550–74559. DOI: https://doi.org/10.1039/c6ra14548e

[52] R. G. Parr, L. V. Szentpály, S. Liu, *J. Am. Chem. Soc.* **1999**, *121*, 1922–1924. DOI: https://doi.org/10.1021/ja983494x

[53] T. Koopmans, *Physica* **1934**, *1 (1–6)*, 104–113.

[54] J. L. Gázquez, A. Cedillo, A. Vela, *J. Phys. Chem. A* **2007**, *111*, 1966–1970. DOI: https://doi.org/10.1021/jp065459f

[55] A. Alverez-Gallegos, D. Pletcher, *Electrochim. Acta* **1999**, *44*, 2483–2492. DOI: https://doi.org/10.1016/S0013-4686(98)00371-5

[56] A. Alvarez-Gallegos, D. Pletcher, *Electrochim. Acta* **1998**, *44 (5)*, 853–861. DOI: https://doi.org/10.1016/S0013-4686(98)00242-4

[57] M. Bhaumik, A. Maity, V. K. Gupta, *J. Colloid Interface Sci.* **2017**, *506*, 403–414. DOI: https://doi.org/10.1016/j.jcis.2017.07.016

[58] F. F. Dias, A. A. S. Oliveira, A. P. Arcanjo, F. C. .C. Moura, J. G. A. Pacheco, *Appl. Catal. B Environ.* **2016**, *186*, 136–142. DOI: https://doi.org/10.1016/j.apcatb.2015.12.049

[59] S. Biton Seror, D. Shamir, Y. Albo, H. Kornweitz, A. Burg, *Chemosphere* **2022**, *286*. DOI: https://doi.org/10.1016/j.chemosphere.2021.131832

[60] M. Vinita, R. Praveena Juliya Dorathi, K. Palanivelu, *Sol. Energy* **2010**, *84*, 1613–1618. DOI: https://doi.org/10.1016/j.solener.2010.06.008

[61] J. J. Pignatello, E. Oliveros, A. MacKay, *Crit. Rev. Environ. Sci. Technol.* **2006**, *36*, 1–84. DOI: https://doi.org/10.1080/10643380500326564

[62] W. G. Kuo, *Water Res.* **1992**, *26*, 881–886. DOI: https://doi.org/10.1016/0043-1354(92)90192-7

[63] J. Chen, L. Zhu, *Chemosphere* **2006**, *65*, 1249–1255. DOI: https://doi.org/10.1016/j.chemosphere.2006.04.016

[64] M. Neamtu, A. Yediler, I. Siminiceanu, A. Kettrup, *J. Photochem. Photobiol. A Chem.* **2003**, *161*, 87–93. DOI: https://doi.org/10.1016/S1010-6030(03)00270-3

[65] R. Saini, M. Kumar Mondal, P. Kumar, *Environ. Prog. Sustainable Energy* **2017**, *36*, 420–427. DOI: https://doi.org/10.1002/ep.12473

[66] H. Zhang, D. Zhang, J. Zhou, *J. Hazard. Mater.* **2006**, *135*, 106–111. DOI: https://doi.org/10.1016/j.jhazmat.2005.11.025

[67] K. C. Namkung, A. E. Burgess, D. H. Bremner, H. Staines, *Ultrason. Sonochem.* **2008**, *15*, 171–176. DOI: https://doi.org/10.1016/j.ultsonch.2007.02.009

[68] M. A. Behnajady, N. Modirshahla, F. Ghanbary, *J. Hazard. Mater.* **2007**, *148*, 98–102. DOI: https://doi.org/10.1016/j.jhazmat.2007.02.003

[69] A. J. Expósito, J. M. Monteagudo, A. Durán, A. Fernández, *Ultrason. Sonochem.* **2017**, *35*, 185–195. DOI: https://doi.org/10.1016/j.ultsonch.2016.09.017

[70] B. Cuiping, G. Wenqi, F. Dexin, X. Mo, Z. Qi, C. Shaohua, G. Zhongxue, Z. Yanshui, *Chem. Eng. J.* **2012**, *197*, 306–313. DOI: https://doi.org/10.1016/j.cej.2012.04.108

[71] O. Primo, M. J. Rivero, I. Ortiz, *J. Hazard. Mater.* **2008**, *153*, 834–842. DOI: https://doi.org/10.1016/j.jhazmat.2007.09.053

[72] R. F. Pupo Nogueira, A. G. Trovó, M. R. A. Da Silva, R. D. Villa, M. C. De Oliveira, *Quim. Nova* **2007**, *30*, 400–408. DOI: https://doi.org/10.1590/S0100-40422007000200030

[73] E. K. Maher, K. N. O'Malley, J. Heffron, J. Huo, B. K. Mayer, Y. Wang, P. J. McNamara, *Chemosphere* **2019**, *220*, 1141–1149. DOI: https://doi.org/10.1016/j.chemosphere.2018.12.161

[74] S. Yildiz, A. Olabi, *Waste Biomass Valorization* **2021**, *12*, 4419–4431. DOI: https://doi.org/10.1007/s12649-020-01334-5

[75] A. Olabi, S. Yildiz, *Environ. Sci. Pollut. Res.* **2021**, *28*, 52565–52575. DOI: https://doi.org/10.1007/s11356-021-14505-1

[76] S. Kaya, C. Kaya, *Mol. Phys.* **2015**, *113*, 1311–1319. DOI: https://doi.org/10.1080/00268976.2014.991771

[77] S. Kaya, C. Kaya, *Comput. Theor. Chem.* **2015**, *1060*, 66–70. DOI: https://doi.org/10.1016/j.comptc.2015.03.004

[78] R. G. Pearson, Hard and Soft Acids and Bases, *J. Am. Chem. Soc.* **1963**, *85*, 3533–3539. DOI: https://doi.org/10.1021/ja00905a001

[79] S. Kaya, C. Kaya, *Inorg. Chem.* **2015**, *54*, 8207–8213. DOI: https://doi.org/10.1021/acs.inorgchem.5b00383